

Both Forward and Reverse TCA Cycles Operate in Green Sulfur Bacteria^{*[S]}

Received for publication, June 23, 2010, and in revised form, July 10, 2010 Published, JBC Papers in Press, July 22, 2010, DOI 10.1074/jbc.M110.157834

Kuo-Hsiang Tang and Robert E. Blankenship¹

From the Departments of Biology and Chemistry, Washington University in St. Louis, St. Louis, Missouri 63130

The anoxygenic green sulfur bacteria (GSBs) assimilate CO₂ autotrophically through the reductive (reverse) tricarboxylic acid (RTCA) cycle. Some organic carbon sources, such as acetate and pyruvate, can be assimilated during the phototrophic growth of the GSBs, in the presence of CO₂ or HCO₃[−]. It has not been established why the inorganic carbon is required for incorporating organic carbon for growth and how the organic carbons are assimilated. In this report, we probed carbon flux during autotrophic and mixotrophic growth of the GSB *Chlorobaculum tepidum*. Our data indicate the following: (a) the RTCA cycle is active during autotrophic and mixotrophic growth; (b) the flux from pyruvate to acetyl-CoA is very low and acetyl-CoA is synthesized through the RTCA cycle and acetate assimilation; (c) pyruvate is largely assimilated through the RTCA cycle; and (d) acetate can be assimilated via both of the RTCA as well as the oxidative (forward) TCA (OTCA) cycle. The OTCA cycle revealed herein may explain better cell growth during mixotrophic growth with acetate, as energy is generated through the OTCA cycle. Furthermore, the genes specific for the OTCA cycle are either absent or down-regulated during phototrophic growth, implying that the OTCA cycle is not complete, and CO₂ is required for the RTCA cycle to produce metabolites in the TCA cycle. Moreover, CO₂ is essential for assimilating acetate and pyruvate through the CO₂-anaplerotic pathway and pyruvate synthesis from acetyl-CoA.

Chlorobaculum tepidum (formerly *Chlorobium tepidum*) (1) is a phototrophic green sulfur bacterium (GSB)² that fixes carbon photoautotrophically through the reductive (reverse) tricarboxylic acid (RTCA) cycle (see Fig. 1A) (2). The RTCA cycle, first reported in a green sulfur bacterium *Chlorobium thiosulfatophilum* (3), is essentially the reversal of the oxidative (forward) tricarboxylic acid (OTCA) cycle. Four enzymes have been recruited for the RTCA cycle to catalyze the reverse reaction of four steps in the OTCA cycle (3); pyruvate:ferredoxin

(Fd) oxidoreductase (acetyl-CoA + CO₂ + 2Fd_{red} + 2H⁺ ⇌ pyruvate + CoA + 2Fd_{ox}), ATP citrate lyase (ACL, acetyl-CoA + oxaloacetate + ADP + P_i ⇌ citrate + CoA + ATP), α-ketoglutarate:ferredoxin oxidoreductase (succinyl-CoA + CO₂ + 2Fd_{red} + 2H⁺ ⇌ α-ketoglutarate + CoA + 2Fd_{ox}) and fumarate reductase (succinate + acceptor ⇌ fumarate + reduced acceptor). Moreover, several GSBs, *C. tepidum* included, are potential mixotrophs that use organic carbon sources for producing biomass in the presence of CO₂ or HCO₃[−] (2, 4, 5).

Fluoroacetate (FAC) is known to be a metabolic poison that is highly toxic to mammals. As a structural analog of acetate, the metabolic pathway of FAC has been suggested to be similar to that of acetate, and the toxicity of FAC can be reduced by acetate (6). FAC is known to be an inhibitor for the OTCA cycle (Fig. 1B). Like acetate, FAC is converted into fluoroacetyl-CoA (7), which condenses with oxaloacetate (OAA) to produce (−)-erythro-(2R,3R)-2-fluorocitrate (2-FC) catalyzed by citrate synthase (CS) (8). It is generally assumed that as (−)-erythro-2-FC is a strong inhibitor of aconitase (9, 10), the metabolic flow of the OTCA cycle is blocked and contributes to the toxicity of FAC. Sirevåg and Ormerod (11) reported decades ago that CO₂ assimilation and carbon flux are affected upon addition of FAC during phototrophic growth of the GSB *Chlorobium limicola*. However, in 2003, Ormerod (12) indicated that it remains to be understood what step of the RTCA cycle is affected by FAC in GSB.

In this report, we address two essential questions: why organic carbon sources, in particular acetate, can enhance the growth of *C. tepidum* (and other GSBs) (5) and why CO₂ (or HCO₃[−]) is required for growth when pyruvate or acetate is assimilated. We present studies of the carbon metabolism and probe the effect of FAC on *C. tepidum* with multiple lines of experimental evidence, including mass spectral analysis of photosynthetic pigments with [¹³C]acetate or pyruvate, physiological studies of FAC, identification of genes for the RTCA cycle, and activity assays for several key enzymes. Throughout this report, an autotrophic culture also supplied with acetate or pyruvate (acetate or pyruvate + HCO₃[−]) is defined as a “mixotrophic” culture, a classification used in a recent review by Kelly and Wood (13).

EXPERIMENTAL PROCEDURES

Materials—Chemicals and enzymes were purchased from Sigma-Aldrich. The ¹³C-labeled acetate and pyruvate were from Cambridge Isotope Laboratories, Inc. The DNA oligomers were from Integrated DNA Technology without further purification.

* This work was supported by Grant NNX08AP62G from the Exobiology Program of NASA (to R. E. B.).

[S] The on-line version of this article (available at <http://www.jbc.org>) contains supplemental Table S1, Figs. S1–S3, and additional references.

¹ To whom correspondence should be addressed: Depts. of Biology and Chemistry, Campus Box 1137, Washington University in St. Louis, St. Louis, MO 63130. Tel.: 314-935-7971; Fax: 314-935-4432; E-mail: blankenship@wustl.edu.

² The abbreviations used are: GSB, green sulfur bacteria; RTCA, reductive (reverse) tricarboxylic acid; ACL, ATP citrate lyase; CS, citrate synthase; FAC, fluoroacetate; 2-FC, 2-fluorocitrate; Bchl c, bacteriochlorophyll c; α-KG, α-ketoglutarate; OAA, oxaloacetate; SDH, succinate dehydrogenase; QRT-PCR, quantitative real-time PCR.

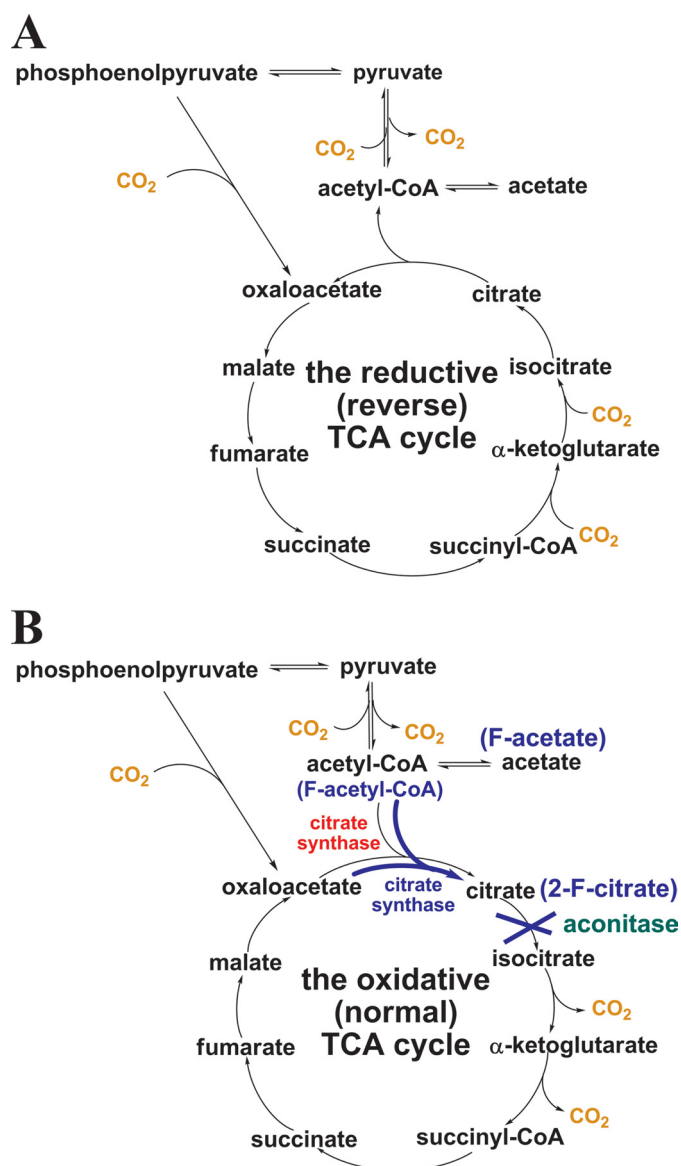


FIGURE 1. Schematic representation of the RTCA cycle (A) and how FAC inhibition occurs in carbon flow via the OTCA cycle (B).

Growth of Bacterial Strains—All *C. tepidum* TLS cultures reported in this work were grown anaerobically at temperatures ranging from 46–50 °C, and cell growth was estimated turbidimetrically at A_{625} . A_{625} was chosen for evaluating the cell growth because absorbance of photosynthetic pigments is minimal ~625 nm (14). The autotrophic and mixotrophic cultures were grown in low intensity light (100 ± 10 micromoles/m²/s), and the list of growth media used in this report and organic carbon sources included in each medium were described previously (2). Typically, 1–2% culture (50–100-fold dilution) in the late exponential growth phase was used to inoculate fresh media.

Determination of Pyruvate, Acetate, and Lactate Concentrations in Cell Cultures—The amount of pyruvate and lactate was determined using the methods reported previously (14–16). The amount of acetate was determined by a coupled acetyl-CoA synthetase/citrate synthase/malate dehydrogenase assay following the formation of NADH (17).

RNA Extraction and Quantitative Real-time PCR (QRT-PCR)

The methods used to extract RNA and perform QRT-PCR were described previously (14, 15, 18). QRT-PCR was performed to profile the gene expression under different growth conditions of *C. tepidum*. The primers for QRT-PCR in this report are listed in supplemental Table S1. Two biological replicates, with three technical replicates for each biological sample, were performed for validation, and the mean value was reported. The amplified DNA fragments were verified by 1% agarose gel electrophoresis, and a single fragment was obtained for all amplicons.

Mass Spectrometry—Photosynthetic pigments in *C. tepidum* cultures were extracted as reported previously (14). The mass spectra of bacteriochlorophyll *c* (Bchl *c*) were acquired using MALDI-TOF mass spectrometry. The MALDI-TOF samples were prepared through mixing a 1:1 volume of sample: matrix (10 mg/ml α -cyano-4-hydroxycinnamic acid in 50% CH₃CN and 0.1% trifluoroacetic acid). Sample measurements were described previously (18). The ¹³C-labeled content of Bchl *c* from mixotrophic cultures with ¹³C-labeled pyruvate or acetate was calculated using the program IsoPro 3.1.

Activity Assays—Enzymatic assays were performed with cell-free crude extracts prepared as follows. Cells were harvested by centrifugation at $5,000 \times g$ for 15 min at 4 °C and washed with 20 mM Tris-HCl buffer at pH 8.0. The cell pellet was resuspended in the same buffer containing 1 mM PMSF. Resuspended cells were disrupted by sonication, and cell debris was removed with centrifugation at $20,000 \times g$ for 30 min. Protein concentration in cell extracts was determined by the Bradford assay (19) using bovine serum albumin as a standard. The enzymatic activities of acetyl-CoA synthetase, acetate kinase, ATP citrate lyase, citrate synthase, P-enolpyruvate carboxykinase, and P-enolpyruvate carboxylase in cell-free extracts were assayed as described previously (20–24).

RESULTS

Pyruvate and Acetate Enhance Growth of *C. tepidum*—It has been well documented that the RTCA cycle is used for CO₂ assimilation when *C. tepidum* grows photoautotrophically. Consistent with previous studies, we have found that photosynthetic pigments are ¹³C-labeled in the autotrophic cultures grown on H¹³CO₃[−] with mass spectrometry (data not shown). To establish conditions for autotrophic or mixotrophic growth of *C. tepidum*, all of the studies for *C. tepidum* carried out in this report were performed in the medium containing 0.34% HCO₃[−] (~40 mM), with or without the inclusion of organic carbon sources. It has been reported that *C. tepidum* photoassimilates acetate or pyruvate (4), and we observed that, compared with autotrophic growth, mixotrophic growth is enhanced ~20% with pyruvate and up to 50% with acetate (Fig. 2A). Additionally, 2–4-fold higher transcript levels were found for most of the genes involved in carbon metabolism during mixotrophic growth compared with autotrophic growth (Table 1). Furthermore, neither acetate nor pyruvate were excreted during autotrophic growth, and at most, 0.2 mM acetate was excreted from the mixotrophic culture with 20 mM pyruvate supplied.

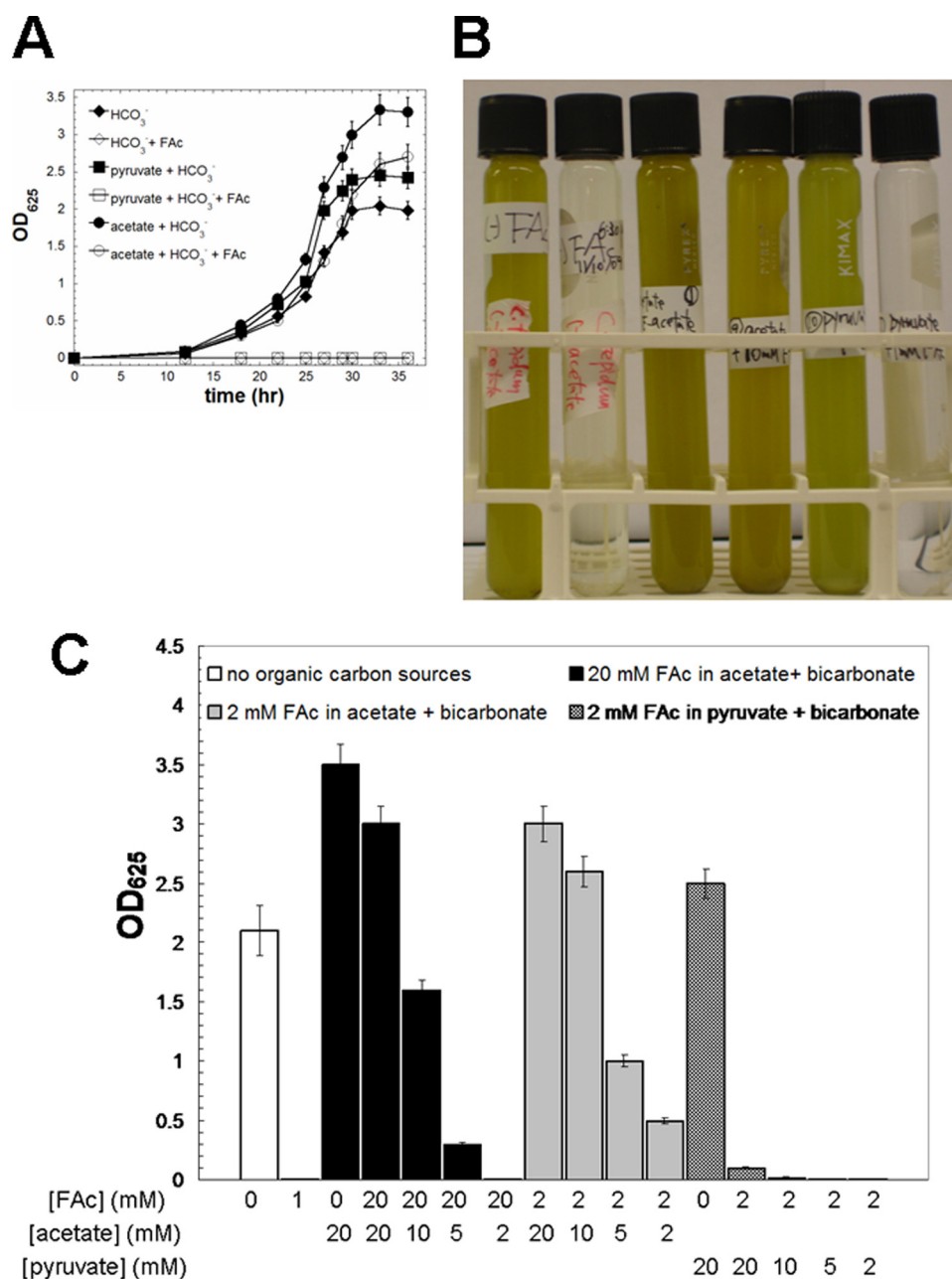


FIGURE 2. **Effect of FAc on the growth of *C. tepidum*.** 0.34% (40 mM) HCO₃⁻ is included in all of the growth media. The growth curve (A) and image of cell cultures (B) of *C. tepidum* during autotrophic and mixotrophic growth (with either 10 mM acetate or pyruvate) conditions with or without 2 mM FAc is shown. The cell growth (recorded as A₆₂₅) during growth conditions with various concentration of acetate, pyruvate, and FAc is shown (C). F, fluoro.

Labeled BChls in the Mixotrophic Cultures with ¹³C-Labeled Acetate or Pyruvate—To probe incorporation of acetate and pyruvate into biomass, we grew cultures of *C. tepidum* with unlabeled or ¹³C-labeled acetate or pyruvate supplied, extracted BChls derived from α-ketoglutarate (α-KG), and acetyl-CoA and examined the molecular mass of Bchl *c* (the major pigment in the chlorosome), with MALDI-TOF. Supplemental Fig. S1 shows that peaks corresponding to the demetallization (M-Mg²⁺ + 2H⁺) of two Bchl *c* isomers, with Δ*m/z* = 14 (C12 substituent as a methyl or ethyl group), were detected and that Bchl *c* was ¹³C-labeled with [¹³C]pyruvate or acetate supplied. Assuming that the carbon number for Bchl *c* in

C. tepidum is 50 or 51 (C₅₀H₆₅N₄O₄ or C₅₁H₆₇N₄O₄ with C17³ farnesyl group and demetallization), the calculated ¹³C-labeled content of Bchl *c* is reported in Table 2. The ¹³C-labeling content was estimated using the program IsoPro 3.1 with the peak at *m/z* 785 and 799 (*m/z* for Bchl *c* with unlabeled carbon sources). Supplemental Fig. S1 and Table 2 indicate slightly higher ¹³C-labeled content of Bchl *c* with [2-¹³C]acetate than with [1-¹³C]acetate and more ¹³C-labeled with [2-¹³C]acetate than with [3-¹³C]pyruvate.

Physiological Studies Using Fluoroacetate—To understand the unidentified role(s) of FAc in the growth of GSB, we set up a series of studies to test the growth of *C. tepidum* with the addition of FAc. Fig. 2A shows that 1 mM FAc is sufficient to inhibit the autotrophic growth of *C. tepidum*. No growth was detected during 36 h of mixotrophic growth with 10 mM pyruvate and 2 mM FAc (Fig. 2B). Even with 20 mM pyruvate and 2 mM FAc, only very slow cell growth was detected after 2 days (A₆₂₅ = ~0.1) (Fig. 2C). Alternatively, significant cell growth can be detected with 10 mM acetate and 2 mM FAc (Fig. 2B) and the transcript levels of genes involved in the RTCA cycle and carbon metabolism are similar with or without FAc added in the mixotrophic culture with acetate (Table 1).

Assimilation of Acetate and FAc—It is generally accepted that acetate assimilation is catalyzed by acetyl-CoA synthetase, for which the activity can be detected in the cell extracts of *C. tepidum* cultures. Using the purified acetyl-CoA synthetase, our kinetic measurements

indicate that FAc is a competitive inhibitor of acetate for acetyl-CoA synthetase and that the catalytic efficiency ratio ((*k*_{cat}/*K*_m)_{acetate} + (*k*_{cat}/*K*_m)_{fluoroacetate})/(*k*_{cat}/*K*_m)_{fluoroacetate} is >400 using the colorimetric assay method reported previously (24). Our results are consistent with the values reported by coupled enzyme assays (25), suggesting that FAc is an alternative and relatively poor substrate for acetyl-CoA synthetase.

Identification of Genes Responsible for the RTCA and OTCA Cycles—In addition to the genes required in the RTCA cycle, *gltA* (CT1834, encoding citrate synthase (CS)) is required for production of citrate in the OTCA cycle and has been annotated in the *C. tepidum* genome (26). Furthermore, two gene

TABLE 1

Relative transcript levels ΔC_T for genes involved in carbon metabolism during autotrophic and mixotrophic growth conditions of *C. tepidum*
 $\Delta C_T = C_T$ (the threshold cycle) of the target gene $- C_T$ of the 16 S rRNA gene.

Gene	Growth condition ^a			
	HCO ₃ ⁻	Pyruvate + HCO ₃ ⁻	Acetate + HCO ₃ ⁻	Acetate + FAc + HCO ₃ ⁻
<i>gltA</i> (CT1834, citrate synthase)	12.8 ± 0.2	11.0 ± 0.1	11.2 ± 0.1	11.4 ± 0.1
<i>aclA</i> (CT1088, ACL, α subunit)	9.4 ± 0.1	8.5 ± 0.2	8.0 ± 0.1	8.3 ± 0.2
<i>aclB</i> (CT1089, ACL, β subunit)	8.6 ± 0.1	7.6 ± 0.1	7.0 ± 0.2	7.8 ± 0.1
<i>porA</i> (CT1628, pyruvate: ferredoxin oxidoreductase)	12.8 ± 0.1	10.5 ± 0.2	11.6 ± 0.2	12.3 ± 0.1
<i>korB</i> (CT0162, KFOR, β subunit)	7.5 ± 0.1	7.2 ± 0.0	7.9 ± 0.2	7.4 ± 0.1
<i>korA</i> (CT0163, KFOR, α subunit)	7.9 ± 0.1	6.2 ± 0.0	7.2 ± 0.1	7.0 ± 0.1
<i>acn</i> (CT0543, aconitase)	8.4 ± 0.1	6.5 ± 0.1	7.3 ± 0.1	8.2 ± 0.1
<i>icd</i> (CT0351, isocitrate dehydrogenase)	8.0 ± 0.2	6.7 ± 0.1	7.2 ± 0.2	7.9 ± 0.2
<i>ppd</i> (CT1682, pyruvate phosphate dikinase)	8.8 ± 0.0	7.6 ± 0.1	7.5 ± 0.0	7.9 ± 0.1
<i>ppc</i> (CT1640, PEP carboxylase)	6.9 ± 0.1	5.4 ± 0.1	6.8 ± 0.2	6.6 ± 0.1
<i>pckA</i> (CT2232, PEP carboxykinase)	7.5 ± 0.1	5.9 ± 0.0	7.7 ± 0.1	7.1 ± 0.3
<i>acsA</i> (CT1652, acetyl-CoA synthetase)	8.6 ± 0.0	6.9 ± 0.2	8.0 ± 0.2	7.8 ± 0.2
<i>ackA</i> (CT1525, acetate kinase)	5.9 ± 0.1	5.7 ± 0.1	6.7 ± 0.1	5.6 ± 0.0
<i>pta</i> (CT1085, phosphotransacetylase)	7.9 ± 0.0	7.8 ± 0.0	8.9 ± 0.0	7.7 ± 0.1

^a Concentrations are as follows: HCO₃⁻ (Na⁺), 0.95 M (8%); and acetate, pyruvate, and FAc, 20 mM each.

^b KFOR, α -ketoglutarate:ferredoxin oxidoreductase; PEP, P-enolpyruvate.

TABLE 2

m/z of BChl *c* with unlabeled or ¹³C-labeled pyruvate or acetate

	<i>m/z</i>	<i>m/z</i>	No. of ¹³ C-labeled carbons ^a	¹³ C-Labeled percentage ^a
Unlabeled pyruvate or acetate	785.6 ^b	799.7 ^b	0	0
[1- ¹³ C]Acetate	790.7	805.7	7–8	14–15
[2- ¹³ C]Acetate	792.8	806.8	8	16
[1- ¹³ C]Pyruvate	786.7	800.7	2	4
[3- ¹³ C]Pyruvate	788.6	802.6	5	10

^a The ¹³C-labeled percentage on BChl *c* was estimated using the program IsoPro 3.1 with molecular masses 785.6 and 799.7 for BChl *c*.

^b The molecular masses 785.6 and 799.7 correspond to the chemical formulas C₅₀H₆₅N₄O₄ and C₅₁H₆₇N₄O₄, with the C17³ farnesyl group and demetallization on BChl *c*.

clusters encoding succinate dehydrogenase (SDH)/fumarate reductase (putative *sdhABC*, CT2040–2042 and CT2266–2268) have also been annotated in the *C. tepidum* genome (26). NADH-dependent fumarate reductase catalyzes the reduction of fumarate to succinate in the RTCA cycle, and SDH catalyzes the oxidation of succinate to fumarate in the OTCA cycle. It is difficult, however, to predict the function of two putative *sdhABC* gene clusters in *C. tepidum* solely from sequence analysis. Additionally, the role of CS in carbon flow of *C. tepidum* has not been understood. To probe the contribution of CS during phototrophic growth of *C. tepidum*, and the functions of two *sdh* gene clusters in *C. tepidum*, we examined the expression level of *gltA* versus *aclAB* (CT1088–1089, encoding both subunits of ATP citrate lyase (ACL; EC 2.3.3.8)) and two sets of the *sdhAB* genes during autotrophic and mixotrophic growth.

Fig. 3A shows the transcriptomic levels of two gene clusters encoding SDH/fumarate reductase after 36 h of autotrophic growth. For two *sdhA*-like genes, the transcript level of CT2042 is ~10-fold higher than that of CT2267, and for two *sdhB*-like genes, CT2041 is ~7-fold higher than CT2266. Because the carbon flux during autotrophic growth is through the RTCA cycle, the *sdhAB*-like genes up-regulated during autotrophic growth most likely encode the fumarate reductase protein. Thus, our data suggest that the CT2040–2242 (or CT2266–2268) during autotrophic growth encode fumarate reductase (or SDH). Similar results were also obtained from mixotrophic growth with pyruvate or acetate (data not shown). Moreover,

SDH/fumarate reductase-like proteins encoded by CT2040–2042, not CT2266–2268, were also reported by recent proteomic studies (27).

Fig. 3A also indicates that the transcript level of *aclAB* is ~6–10-fold higher than *gltA*. The CS protein has been previously reported by the proteomic analysis of *C. tepidum* (27, 28), and the studies by Hosoya-Matsuda *et al.* (28) suggested that CS is inactivated under conditions when ACL is activated. Consistent with their working hypothesis, the enzymatic activity of ACL, not that of CS, can be detected in cell extracts of autotrophic and mixotrophic growth cultures (Fig. 3B and supplemental Fig. S3). Furthermore, we probed the gene expression level of *gltA* during different stages of the mixotrophic growth with acetate. Fig. 3C shows the gene expression level of *gltA* versus some essential genes for the RTCA cycle. *aclAB* versus *gltA*, *aclA* (encoding the large subunit of ACL) versus *acn* (encoding aconitase), and *aclA* versus *korA* (encoding the α -subunit of α -keto-glutarate:ferredoxin oxidoreductase). The relative expression level of *aclA/gltA* and *aclB/gltA* is lower during the lag phase and early log phase of the growth and is higher during the late log phase and stationary phase of the growth. In comparison, the relative expression level of *aclA* versus *acn* and *aclA* versus *korA* is similar during the growth period.

Taken together, the transcriptomic analysis and activity assays described above indicate that the major carbon flux during both autotrophic and mixotrophic growth of *C. tepidum* is through the RTCA cycle. Additionally, the partial OTCA cycle may also contribute to the carbon flux of *C. tepidum* during mixotrophic growth with acetate, as considered under “Discussion.”

DISCUSSION

Carbon Flow during Mixotrophic Growth of *C. tepidum*—Although it has been well established that the RTCA cycle is employed during autotrophic growth of GSBs, the carbon flow during mixotrophic growth has not been understood. To address this unresolved and essential issue, we analyze the multiple lines of evidence listed below for the mixotrophic growth of *C. tepidum* with acetate or pyruvate.

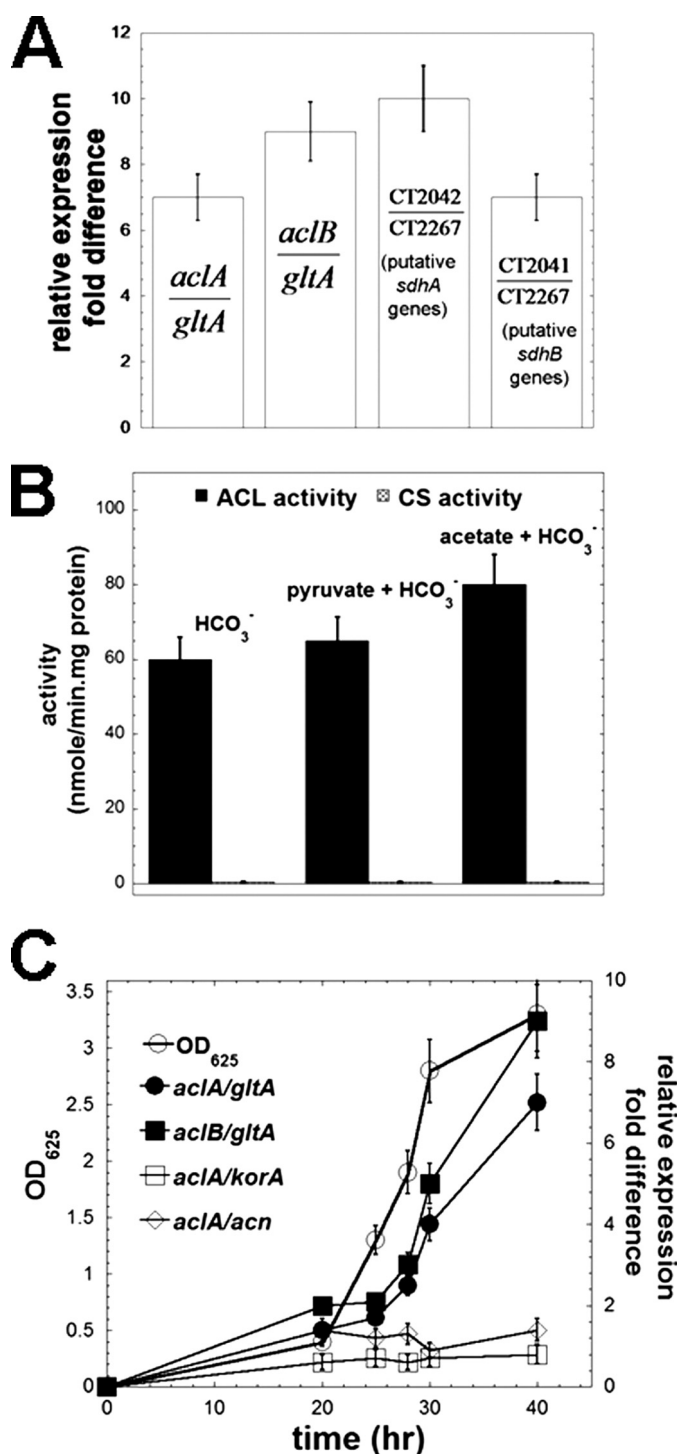


FIGURE 3. Shown are gene expression profiles for ACL (subunits A and B are encoded by *aclA* and *aclB*, respectively), CS (encoded by *gltA*), and putative succinate dehydrogenase/fumarate reductase subunit A (*sdhA*) and subunit B (*sdhB*) of *C. tepidum*, and activity assays for ACL and CS. Relative gene expression profiles of *aclA/gltA*, *aclB/gltA*, CT2042/CT2267 (putative *sdhA*), and CT2041/CT2267 (putative *sdhB*) after 36 h of autotrophic growth (A), the enzymatic activity of ACL and CS in autotrophic and mixotrophic cultures (B), and relative gene expression levels of *aclA/gltA*, *aclB/gltA*, *aclA/acn* (*acn* encoding aconitase) and *aclA/korA* (*korA* encoding α -keto-glutarate:ferredoxin oxidoreductase, α subunit) during various growth stages of mixotrophic cultures with 10 mM acetate are shown (C). The data in this figure were acquired from experiments performed two times in triplicate, and the error bar is the standard deviation of the mean value.

Labeled BChls with ^{13}C -Labeled Acetate or Pyruvate—Biosynthesis of (B)Chls requires eight glutamate molecules for forming the Mg^{2+} -chelating tetrapyrrole ring and several molecules of acetyl-CoA for synthesizing the hydrophobic tail.

If pyruvate is assimilated mainly through the OTCA cycle, acetyl-CoA, α -KG, and BChls will not be labeled using [$1\text{-}^{13}\text{C}$]pyruvate. Alternatively, acetyl-CoA (from cleavage of citrate), α -KG, and BChls are expected to be labeled with [$1\text{-}^{13}\text{C}$]pyruvate through the RTCA cycle (supplemental Fig. S3A). Our studies show that two to three carbons were ^{13}C -labeled with [$1\text{-}^{13}\text{C}$]pyruvate (Table 2 and supplemental Fig. S1D). Less ^{13}C -enriched BChl *c* can be attributed to fast exchange between pyruvate and acetyl-CoA catalyzed by pyruvate:ferredoxin oxidoreductase and/or ^{13}C -labeled scrambled in succinate.

Moreover, Table 2 and supplemental Fig. S1 indicate more ^{13}C -labeled content of BChl *c* with [$2\text{-}^{13}\text{C}$]acetate (16%) than with [$3\text{-}^{13}\text{C}$]pyruvate (10%). Both α -KG and acetyl-CoA contribute to ^{13}C -labeled BChl *c*, and acetyl-CoA is labeled through the RTCA cycle with [$2\text{-}^{13}\text{C}$]acetate or [$3\text{-}^{13}\text{C}$]pyruvate (supplemental Fig. S3B). Thus, if acetate and pyruvate are photoassimilated exclusively via the RTCA cycle, similar ^{13}C -labeled content of BChl *c* is expected with [$2\text{-}^{13}\text{C}$]acetate versus [$3\text{-}^{13}\text{C}$]pyruvate. We propose that higher ^{13}C -labeled content of BChl *c* with [$2\text{-}^{13}\text{C}$]acetate is acquired because acetate is assimilated through both RTCA and OTCA cycles, and more ^{13}C -labeled α -KG is obtained through the OTCA cycle (supplemental Fig. S3B). This hypothesis is supported by our FAc studies, as discussed next.

The Studies of FAc—Fig. 2 shows significant inhibition by 2 mM FAc during the mixotrophic growth of *C. tepidum* with 20 mM pyruvate and less inhibition by FAc during mixotrophic growth with acetate. These results imply that during mixotrophic growth with pyruvate, the metabolic flux favors the formation of P-enolpyruvate (Fig. 4A). With less acetyl-CoA generated from pyruvate to compete with fluoroacetyl-CoA from FAc, the mixotrophic growth with pyruvate is expected to be repressed (Fig. 4C). Alternatively, our studies show that acetate is a much better substrate than FAc for acetyl-CoA synthetase (see “Results”), consistent with less FAc inhibition during mixotrophic growth with acetate (Fig. 2).

From the mechanism of action of FAc reported in other organisms, we propose that the inhibition by FAc for the growth of *C. limicola* and *C. tepidum* arises from the formation of (–)-erythro-2-FC that blocks the carbon flux of the RTCA cycle. It has not been reported whether (–)-erythro-2-FC can be generated from FAc through the RTCA cycle. Alternatively, (–)-erythro-2-FC may be catalyzed by ACL or/and CS (as discussed below). In contrast, we cannot detect FAc-inhibition in the pyruvate- or acetate-grown photoheterotrophic bacterium *Heliobacterium modesticaldum*, in which no genes encoding ACL or CS have been annotated (29), and no activity of ACL or CS has been detected (14). Together, two conclusions can be reached with the physiological studies of FAc for *C. tepidum*. One is that low flux from pyruvate to acetyl-CoA and acetyl-CoA is mainly generated in *C. tepidum* through acetate uptake and the RTCA cycle. Thus, acetyl-CoA production is prohibited through the RTCA cycle when aconitase is inhibited

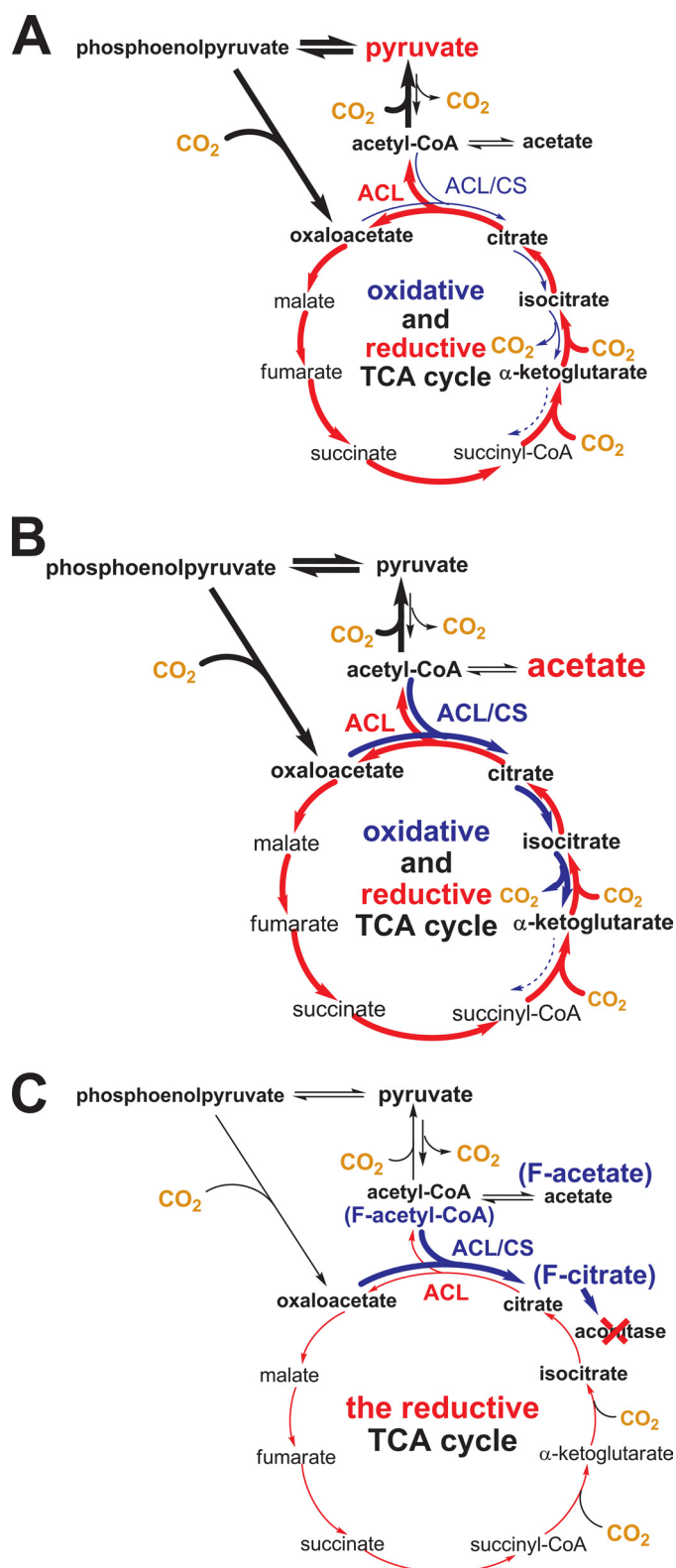
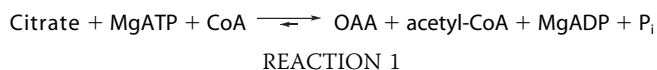


FIGURE 4. **The proposed carbon flux in *C. tepidum*.** The proposed carbon flux during mixotrophic growth with pyruvate (A) and acetate (B) and the proposed FAc effect for the carbon flux (C). F, fluoro.

upon addition of FAc. The other conclusion is some of the carbon fluxes through the OTCA cycle during the mixotrophic growth with acetate, consistent with mass spectral evidence presented in this report.

Possible Roles of ACL and CS—As annotated in the *C. tepidum* genome, genes encoding CS (Clim_2042) and both subunits of ACL (Clim_1231 and Clim_1232) have also been annotated in the *C. limicola* genome. The roles of ACL and CS in GSBs are discussed as follows.

The enzymatic activity of ACL can be detected in the cell extracts of *C. tepidum* (Fig. 3B and supplemental Fig. S3). The reaction catalyzed by ACL is shown below.



Note that ACL cleaves the acetyl-moiety in the “pro-S arm” of citrate to produce acetyl-CoA, which is the reverse reaction catalyzed by the common CS (or (Si)-CS). Thus, if the reaction catalyzed by ACL is reversible, ACL may catalyze the formation of (–)-erythro-2-FC from condensation of fluoroacetyl-CoA and OAA during the phototrophic growth of *C. tepidum*. Although the recombinant ACL from *C. limicola* was reported to catalyze only the cleavage of citrate (30), ACL isolated from rat liver (31) and several prokaryotic ACL enzymes can catalyze both citrate cleavage and citrate formation through condensation of OAA and acetyl-CoA (32, 33). Moreover, many enzyme-catalyzed aldol/retro-aldol reactions, such as fructose 1,6-bisphosphate aldolase and transketolases, are reversible both *in vivo* and *in vitro*. The recombinant ACL from *C. tepidum* has been characterized biochemically (20). If the reaction catalyzed by *C. tepidum* ACL is reversible, citrate can be generated along with ATP through substrate-level phosphorylation, which may provide one of the rationales for better mixotrophic growth with acetate than with pyruvate.

CS has been recognized for catalyzing the formation of (–)-erythro-2-FC from OAA and fluoroacetyl-CoA for the inhibition of aconitase (10), and fluoroacetyl-CoA and acetyl-CoA have been shown to have similar reactivity with CS (7). Previous studies in *C. tepidum* indicated that CS is inactivated under conditions in which ACL is activated and vice versa (28). Consistent with this hypothesis, our studies show that the relative gene expression level of *gltA/aclA* is higher in the earlier stage than in the late stage of the growth and that the transcript level of *gltA* is higher during acetate uptake and is lower when acetate is assimilated (Fig. 3C). Thus, although the activity of CS has neither been detected previously (28) nor in our hands (supplemental Fig. S2), one cannot rule out the contribution of CS during phototrophic growth of *C. tepidum*. The role of CS is currently being investigated with the ΔgltA mutant of *C. tepidum*.

Requirement of CO_2 for Growth of *C. tepidum* with Organic Carbon—In contrast to heterotrophs, acetate or pyruvate can enhance but cannot be used as a sole carbon source without including CO_2 or HCO_3^- during the growth of GSBs (2, 5). The enzymatic activities of four enzymes responsible for CO_2 assimilation in the RTCA cycle were reported in the GSB *C. thiosulfatophilum* (3, 34) (now *Chlorobaculum thiosulfatophilum*) (1), and we also detected the enzymatic activities of P-enolpyruvate carboxylase and P-enolpyruvate carboxykinase (25–40 nmol/min·mg protein) in cell extracts of the autotrophic and mixotrophic cultures of *C. tepidum*. Together, previ-

ous and our studies suggest that the CO₂-anaplerotic pathway is active during phototrophic growth of GSBs. The contribution of the CO₂-anaplerotic pathway to the carbon metabolism of photoheterotrophic bacteria has also been identified experimentally (14, 15). Thus, in addition to being required for the RTCA cycle, CO₂ is essential for assimilating pyruvate and acetate through the CO₂-anaplerotic pathway and incorporating acetate through the catalysis of pyruvate:ferredoxin oxidoreductase (acetyl-CoA + CO₂ + 2Fd_{red} + 2H⁺ → pyruvate + CoA + 2Fd_{ox}) (Fig. 4).

Although the activities for all of the enzymes in the RTCA cycle have been identified (3), the genes specific for the OTCA cycle are either absent (*pdhAB* for pyruvate dehydrogenase and *sucAB* for α-ketoglutarate dehydrogenase) in the *C. tepidum* genome or down-regulated (*gltA* for CS and CT2266–2268 for SDH) during phototrophic growth (Fig. 3A). Thus, only a partial OTCA cycle is expected to be employed by *C. tepidum* growing phototrophically. The proposed partial OTCA cycle is likely to go through citrate to α-KG because the reactions catalyzed by aconitase and isocitrate dehydrogenase are reversible (35, 36), and α-keto-glutarate:ferredoxin oxidoreductase is more favorable for catalyzing reductive carboxylation of α-KG. Thus, CO₂ is required for the RTCA cycle to produce intermediates in the TCA cycle for biosynthetic pathways (Fig. 4).

CONCLUSIONS

Although GSBs are known to produce biomass through assimilating CO₂ via the RTCA cycle, the carbon flow during autotrophic and mixotrophic growth has not been fully understood. Here, we report studies of carbon flow of *C. tepidum* with multiple lines of experimental evidence, including mass spectral analysis of Bchl *c* with [¹³C]acetate or pyruvate, physiological studies of FAC, identification of genes for the RTCA cycle, and activity assays for several key enzymes. Our studies demonstrate that *C. tepidum* utilizes not only the RTCA cycle but also the OTCA cycle that has not been revealed previously, consistent with the metabolic flux analysis of *C. tepidum*.³

Acknowledgments—We thank Dr. Jianzhong Wen for assistance in acquiring the mass spectra in [supplemental Fig. S1](#), Barbara Honchak for proofreading the revised manuscript, and Xueyang Feng and Dr. Yinjie Tang for discussions.

REFERENCES

- Imhoff, J. F., and Thiel, V. (2010) *Photosynth. Res.* **104**, 123–136
- Overmann, J. (2006) *The Prokaryotes* 3rd Ed., Vol. 7, pp. 359–378, Springer, New York
- Evans, M. C., Buchanan, B. B., and Arnon, D. I. (1966) *Proc. Natl. Acad. Sci. U.S.A.* **55**, 928–934
- Wahlund, T. M., Woese, C. R., Castenholz, R. W., and Madigan, M. T. (1991) *Arch. Microbiol.* **156**, 81–90
- Sadler, W. R., and Stanier, R. Y. (1960) *Proc. Natl. Acad. Sci. U.S.A.* **46**,

- 1328–1334
- Gribble, G. W. (1973) *J. Chem. Educ.* **50**, 460–462
- Marcus, A., and Elliott, W. B. (1956) *J. Biol. Chem.* **218**, 823–830
- Proudfoot, A. T., Bradberry, S. M., and Vale, J. A. (2006) *Toxicol. Rev.* **25**, 213–219
- Lauble, H., Kennedy, M. C., Emptage, M. H., Beinert, H., and Stout, C. D. (1996) *Proc. Natl. Acad. Sci. U.S.A.* **93**, 13699–13703
- Villafranca, J. J., and Platus, E. (1973) *Biochem. Biophys. Res. Commun.* **55**, 1197–1207
- Sirevag, R., and Ormerod, J. G. (1970) *Science* **169**, 186–188
- Ormerod, J. (2003) *Photosynth. Res.* **76**, 135–143
- Kelly, D. P., and Wood, A. P. (2006) *The Prokaryotes*, 3rd Ed., Vol. 2, pp. 441–456, Springer, New York
- Tang, K. H., Yue, H., and Blankenship, R. E. (2010) *BMC Microbiol.* **10**, 150
- Tang, K. H., Feng, X., Tang, Y. J., and Blankenship, R. E. (2009) *PLoS One* **4**, e7233
- Howell, B. F., McCune, S., and Schaffer, R. (1979) *Clin. Chem.* **25**, 269–272
- Ma, K., Hutchins, A., Sung, S. J., and Adams, M. W. (1997) *Proc. Natl. Acad. Sci. U.S.A.* **94**, 9608–9613
- Tang, K. H., Wen, J., Li, X., and Blankenship, R. E. (2009) *J. Bacteriol.* **191**, 3580–3587
- Bradford, M. M. (1976) *Anal. Biochem.* **72**, 248–254
- Kim, W., and Tabita, F. R. (2006) *J. Bacteriol.* **188**, 6544–6552
- Chen, Z. H., Walker, R. P., Técsi, L. I., Lea, P. J., and Leegood, R. C. (2004) *Planta* **219**, 48–58
- Pickett, M. W., Williamson, M. P., and Kelly, D. J. (1994) *Photosynth. Res.* **41**, 75–88
- Kumari, S., Tishel, R., Eisenbach, M., and Wolfe, A. J. (1995) *J. Bacteriol.* **177**, 2878–2886
- Kuang, Y., Salem, N., Wang, F., Schomisch, S. J., Chandramouli, V., and Lee, Z. (2007) *J. Biochem. Biophys. Methods* **70**, 649–655
- Patel, S. S., and Walt, D. R. (1987) *J. Biol. Chem.* **262**, 7132–7134
- Eisen, J. A., Nelson, K. E., Paulsen, I. T., Heidelberg, J. F., Wu, M., Dodson, R. J., Deboy, R., Gwinn, M. L., Nelson, W. C., Haft, D. H., Hickey, E. K., Peterson, J. D., Durkin, A. S., Kolonay, J. L., Yang, F., Holt, I., Umayam, L. A., Mason, T., Brenner, M., Shea, T. P., Parksey, D., Nierman, W. C., Feldblyum, T. V., Hansen, C. L., Craven, M. B., Radune, D., Vamathevan, J., Khouri, H., White, O., Gruber, T. M., Ketchum, K. A., Venter, J. C., Tettelin, H., Bryant, D. A., and Fraser, C. M. (2002) *Proc. Natl. Acad. Sci. U.S.A.* **99**, 9509–9514
- Kouyianou, K., Aivaliotis, M., Gevaert, K., Karas, M., and Tsiotis, G. (2010) *Photosynth. Res.* **104**, 153–162
- Hosoya-Matsuda, N., Inoue, K., and Hisabori, T. (2009) *Mol. Plant.* **2**, 336–343
- Sattley, W. M., Madigan, M. T., Swingle, W. D., Cheung, P. C., Clocksin, K. M., Conrad, A. L., Dejesa, L. C., Honchak, B. M., Jung, D. O., Karbach, L. E., Kurdoglu, A., Lahiri, S., Mastrian, S. D., Page, L. E., Taylor, H. L., Wang, Z. T., Raymond, J., Chen, M., Blankenship, R. E., and Touchman, J. W. (2008) *J. Bacteriol.* **190**, 4687–4696
- Kanao, T., Fukui, T., Atomi, H., and Imanaka, T. (2002) *Eur. J. Biochem.* **269**, 3409–3416
- Inoue, H., Suzuki, F., Tanioka, H., and Takeda, Y. (1968) *J. Biochem.* **63**, 89–100
- Moller, D., Schauder, R., Fuchs, G., and Thauer, R. K. (1987) *Arch. Microbiol.* **148**, 202–207
- Beh, M., Strauss, G., Huber, R., Stetter, K. O., and Fuchs, G. (1993) *Arch. Microbiol.* **160**, 306–311
- Evans, M. C., Buchanan, B. B., and Arnon, D. I. (1966) *Science* **152**, 673
- Kanao, T., Kawamura, M., Fukui, T., Atomi, H., and Imanaka, T. (2002) *Eur. J. Biochem.* **269**, 1926–1931
- Lebedeva, N. V., Malinina, N. V., and Ivanovsky, R. N. (2002) *Microbiology* **71**, 657–661

³ X. Feng, K. H. Tang, R. E. Blankenship, and Y. J. Tang, submitted for publication.